Published in final edited form as:
Brain Res. 2007 October 10; 1173: 66–77.

Early segregation of layered projections from the lateral superior olivary nucleusto the central nucleus of the inferior colliculus in the neonatal cat

Mark L. Gabriele[1,*], **Sarah H. Shahmoradian**[1], **Christopher C. French**[1], **Craig K.we Henkel**[2], and **John G. McHaffie**[2]

1 *James Madison University, Department of Biology, MSC 7801, Harrisonburg, VA 22807*

2 *Wake Forest University School of Medicine, Department of Neurobiology and Anatomy, Winston-Salem, North Carolina 27157-1010*

Abstract

The central nucleus of the inferior colliculus (IC) is a laminated structure that receives multiple converging afferent projections. These projections terminate in a layered arrangement and are aligned with dendritic arbors of the predominant disc-shaped neurons, forming fibrodendritic laminae. Within this structural framework, inputs terminate in a precise manner, establishing a mosaic of partially overlapping domains that likely define functional compartments. Although several of these patterned inputs have been described in the adult, relatively little is known about their organization prior to hearing onset. The present study used the lipophilic carbocyanine dyes DiI and DiD to examine the ipsilateral and contralateral projections from the lateral superior olivary (LSO) nucleus to the IC in a developmental series of paraformaldehyde-fixed kitten tissue. By birth, the crossed and uncrossed projections had reached the IC and were distributed across the frequency axis of the central nucleus. At this earliest postnatal stage, projections already exhibited a characteristic banded arrangement similar to that described in the adult. The heaviest terminal fields of the two inputs were always complementary in nature, with the ipsilateral input appearing slightly denser. This early arrangement of interdigitating ipsilateral and contralateral LSO axonal bands that occupy adjacent sublayers supports the idea that the initial establishment of this highly organized mosaic of inputs that defines distinct synaptic domains within the IC occurs largely in the absence of auditory experience. Potential developmental mechanisms that may shape these highly ordered inputs prior to hearing onset are discussed.

Keywords

auditory midbrain; lateral superior olive; inferior colliculus; development; fibrodendritic laminae; DiI

1. Introduction

The central nucleus of the inferior colliculus (IC) is the site of convergence for multiple ascending auditory pathways en route to higher centers of thalamus and cortex (Osen,

* Mail Correspondence to: Dr. Mark L. Gabriele, Ph.D., Associate Professor, James Madison University, Department of Biology, MSC 7801, Harrisonburg, Virginia 22807, phone: (540) 568-6333, fax: (540) 568-3333, email: gabrieml@jmu.edu

1972;Beyerl, 1978;Elverland, 1978;Roth et al., 1978;Adams, 1979;Brunso-Bechtold et al., 1981;Zook and Casseday, 1982;Henkel and Spangler, 1983;Oliver, 1987a;Shneiderman and Henkel, 1987;Shneiderman et al., 1988;Oliver et al., 1995). Its seemingly homogeneous appearance with routine cell staining belies the underlying complexity of the central nucleus. In fact, several levels of organization are now known to exist, from its well-documented arrangement of fibrodendritic laminae (Morest, 1964;Morest and Oliver, 1984;Oliver and Morest, 1984;Faye-Lund and Osen, 1985) to a finer-scale mosaic arrangement of anatomical and functional compartments that together reveal the intrinsic synaptic circuitry (for review see Oliver, 2005). The fibrodendritic laminae that provide the framework for the subsequent levels of organization are composed of sheets of neurons exhibiting disc-shaped dendritic arbors that are aligned with each other and with respect to associated afferent layers (Oliver and Morest, 1984). Functionally, these fibrodendritic laminae preserve the tonotopic map established in the cochlea. Many of the major ascending pathways, including those originating from the cochlear nuclei, the superior olivary complex, and the nuclei of the lateral lemniscus, exhibit a banded distribution consisting of alternating axonal layers with intervening gaps (Shneiderman and Henkel, 1987;Henkel and Shneiderman, 1988;Oliver et al., 1997;Loftus et al., 2004;Malmierca et al., 2005). While most of these individual inputs share a general banded appearance in coronal sections through the IC, not all end uniformly in all layers (e.g. the medial superior olive, MSO, preferentially targets low-frequency laminae) or even within a given layer. For example, crossed inputs from the dorsal cochlear nucleus (DCN) distribute fully along the ventrolateral-to-dorsomedial extent of their target layers, forming complete afferent bands. In contrast, inputs from the lateral superior olive (LSO) and the dorsal nucleus of the lateral lemniscus (DNLL) have more focused terminal fields within their target layers and thus end in shorter bands or multiple patches concentrated in a part of the layer (Shneiderman and Henkel, 1987;Henkel and Shneiderman, 1988;Oliver et al., 1997;Gabriele et al., 2000a). With the varying array of inputs and the partial overlap of many of these projections, a single fibrodendritic lamina within the central nucleus likely contains groups of neurons that receive different combinations of inputs, demonstrate different response profiles (Merzenich and Reid, 1974;Semple and Aitkin, 1979;Schreiner and Langner, 1997), and therefore are capable of processing different auditory information.

The adult distribution of afferent projections to the central nucleus of the IC has been described in a variety of species. Projections arising from the cochlear nuclei (Oliver 1984;Oliver, 1987b;Oliver et al., 1997;Malmierca et al., 2005), the LSO (Shneiderman and Henkel, 1987;Oliver et al., 1997;Loftus et al., 2004), and the DNLL (Kudo, 1981;Tanaka et al., 1985;Zook and Casseday, 1987;Shneiderman et al., 1988) are among the most banded inputs to the IC and have therefore received the most attention. Shneiderman and Henkel (1987) were the first to describe the direct spatial relationship of two banded inputs within the central nucleus. The ipsilateral inhibitory LSO projection was shown to form complementary bands and patches that interdigitate with the excitatory input that arises from the contralateral LSO. More recently, a series of double-labeling studies in the adult cat has provided significant insights concerning the convergence onto individual laminae of axonal projections from different brainstem auditory nuclei (Oliver et al., 1997;Loftus et al., 2004;Malmierca et al., 2005). By carefully matching localized injections in similar characteristic frequency domains of different brainstem nuclei, they were able to describe the relation of multiple projections that share mutual layers in the central nucleus of the IC. For instance, projections originating in the contralateral DCN and the LSO target the same sublayers of individual fibrodendritic laminae and are superimposed with each other in the ventrolateral region of the sublayer (Oliver et al., 1997). Filling in the gaps in adjacent sublayers are the inputs from the ipsilateral LSO (Shneiderman and Henkel, 1987) that overlap in part with the ipsilateral MSO projection in more lateral, low frequency regions of the central nucleus (Loftus et al., 2004). Finally, calcium-binding proteins, specifically calbindin-D28k in the adult cat (Henkel et al., 2005), may serve as convenient neurochemical markers during early development for labeling certain

layered inputs to the IC. The partial overlap and non-overlap of these various developmental patterns are thought to determine the innervation and organizational scheme for functional compartments of neurons within the central nucleus of the IC.

Since patterns of afferent projections to the IC define functional compartments and determine the types of processing that occur within fibrodendritic layers, it is essential to understand the manner in which these patterns are established and subsequently shaped. To date, the majority of developmental studies addressing these issues have been performed in rat (Kandler and Friauf, 1993;Okoyama et al., 1995;Gabriele et al., 2000a;Gabriele et al., 2000b). Kandler and Friauf (1993) described the developmental progression of the projection arising from the cochlear nucleus. While a detailed temporal account of periods of fiber outgrowth, axonal arrival, and collateral branching within the contralateral IC was well-documented, there was little mention of the shaping of cochlear nucleus projections into their characteristic banded appearance. More recently, we described the development of the crossed DNLL projection in pre- and postnatal rat tissue (Gabriele et al., 2000a). The results of this study indicated that the adult-like pattern of DNLL bands and subsequent patches that develop do so from an initially diffuse distribution. DNLL bands are detectable by postnatal day 4 (P4) and are fully refined a week later by the onset of hearing. While spontaneous activity levels that are generated in the periphery during this period (Lippe, 1994;Lippe, 1995;Kotak and Sanes, 1995;Jones et al., 2001) have been shown to influence development of afferent bands (Gabriele et al., 2000b;Franklin et al., 2005), it is likely that other mechanisms (e.g. molecular signaling through receptor-ligand interactions) aid developing projections in defining appropriate terminal zones within the central nucleus (Gabriele et al., 2005).

The present experiments were intended to provide a qualitative assay of the salient features for the developing crossed and uncrossed LSO projections. Of particular interest was to determine whether a complementary pattern of LSO bands is detectable in the IC prior to the onset of hearing. Preliminary aspects of this paper have been published previously in abstract form (Gabriele et al., 2005).

2. Results

2.1 Single-labeling studies

Unilateral placements of DiI were made in the left LSO in a developmental series of early postnatal kitten tissue. Dye deposits were large, labeling substantial regions of the LSO (Fig. 1A) while not significantly compromising the neighboring MSO and periolivary nuclei. Extensive retrograde labeling of cell bodies in the MNTB (Fig. 1A) and the anterior ventral cochlear nucleus (AVCN, Fig. 1B) provided additional confirmation of accurate tracer placements in the LSO. These retrograde data in the newborn animal suggest that connections between the cochlear nuclear and superior olivary complexes, as well as connections within the superior olivary complex itself, are established prenatally.

Even in the youngest animals studied, anterograde labeling of the crossed and uncrossed LSO projections was evident within the central nucleus of the IC (Fig. 2). By birth, axons invaded the central nucleus, distributed across the entirety of its frequency axis, and exhibited numerous branch points, suggesting that the initial period of collateralization takes place prenatally. Parental fibers at this age showed a distinct laminar bias that paralleled that of fibrodendritic laminae, terminating in a ventrolateral to dorsomedial fashion. While some fibers distributed in the central nucleus along the entire ventrolateral to dorsomedial extent of the layers up to the boundary with the deepest layers of the dorsal cortex, most axons were already concentrated in more focal regions of the layers characteristic of the adult-like distribution of LSO projections. Labeled afferents were not uniformly distributed across the laminae within the central nucleus, but rather preferentially targeted alternating sublayers, forming a repetitive

pattern of afferent dense layers (arrowheads, Fig. 2A and Fig. 2B) interspersed with layers with far more sparse labeling. This pattern of afferent bands was readily apparent in both the ipsilateral and contralateral IC. At P0, labeled afferent bands exhibited an approximate thickness of 75–100μm, considerably less than the range of 150 – 200μm reported for the adult IC (Shneiderman and Henkel, 1987;Oliver and Huerta, 1992;Henkel et al., 2005;Malmierca et al., 2005).

Qualitative observations of anterograde DiI labeling suggest that the crossed and uncrossed LSO projections exhibit regular, periodic spacing parallel to IC layers at each of the developmental stages studied. The uncrossed projection was reliably labeled in all cases and routinely appeared slightly denser than the resultant labeling of the crossed projections. Banding for the uncrossed projection was well established at birth (d-value = 0.00006; Fig 3A series). Similar banding scores for the uncrossed input were seen at each of the subsequent ages. At P4, bands continued to be readily discernible (d-value = 0.00037) and slightly thicker, measuring consistently in the range of 100 – 125μm (Fig. 3B series). Ipsilateral LSO afferent bands remained prominent more than a week after birth (Fig. 3C series; d-value = 0.00009) and approached a thickness of 150μm, equal to the lower limit described for IC afferent bands in the adult.

The course that crossed LSO axons travel to reach the contralateral IC is longer than that for ipsilaterally projecting fibers. In a few older unilateral cases, substantial labeling was observed in the ipsilateral IC while crossed fibers appeared to stop in the dorsal aspects of the lateral lemniscus just short of the contralateral IC. Since multiple cases at younger ages yielded reliable contralateral IC data, it is likely that in these few instances not enough time was allotted for adequate diffusion of the dye to facilitate full labeling of the crossed projection. Thus, in the remaining P10 and P14 tissue blocks an additional month incubation time was given to ensure complete filling of the crossed axonal arbors. The results indicate that the crossed projection, much like its uncrossed counterpart, yielded significant periodicity scores at each of the studied stages (Fig. 4A–4C series). Contralateral labeling, however, was usually slightly less dense than the corresponding ipsilateral input. No qualitative differences were seen in the relative thickness of the ipsilateral and contralateral bands at the various stages, suggesting that the two inputs grow in a similar fashion during the first two postnatal weeks. As expected, large dye placements in the LSO resulted in numerous labeled bands spanning the frequency axis of the central nucleus (Fig 4A series; d-value = 0.00054). In contrast, cases with more focal LSO dye placements yielded comparatively fewer labeled bands in the IC (Figure 4B series; d-value = 0.00081). In this particular case the previously described two-winged morphology of an individual afferent layer was observed (Shneiderman and Henkel, 1987;Oliver et al., 1997;Loftus et al., 2004). The prominent, more medial wing (Fig. 4B *arrowhead*) was located in *pars centralis*, while the more lateral limb (Fig. 4B *arrow*) was located in *pars lateralis* subdivision of the central nucleus. Just as the more medial limb exhibited the ventrolateral-to-dorsomedial orientation of the laminae in *pars centralis*, the limb situated in *pars lateralis* was arranged in its characteristic orthogonal orientation to the laminae of *pars centralis* (Oliver and Morest, 1984). By P7, boundaries of the contralateral afferent band were clearly delineated (Fig. 4C series; d-value = 0.00131), with very little labeling still present in the alternating interband spaces.

2.2 Double-labeling studies: Interdigitation of the crossed and uncrossed LSO inputs

Simultaneous placements of DiI and DiD were made in the left and right LSO (Fig. 5), with the dye-coated pins positioned to facilitate maximal labeling of the crossed and uncrossed pathways. The result confirmed findings from the described unilateral cases, while also providing novel double-labeling data for observations regarding the segregation and interdigitation of the developing crossed and uncrossed inputs.

Following bilateral dye placements in even the youngest animals studied, patterns for both the crossed and uncrossed labeled projections were observed in each IC. At each of the ages studied, a striking pattern of interdigitating ipsilateral and contralateral inputs was evident (Fig. 6). At selected rostrocaudal levels where axonal layers were most prominent, multiple images of the same field of view were captured utilizing the filter sets optimized for DiI (Fig. 6A), DiD (Fig. 6B), and the particular counterstain (Fig. 6C). A digitally merged image (Fig. 6D) facilitated study of the spatial relationships of the crossed and uncrossed projection patterns. It is clear that by birth the projections originating in the contralateral LSO and the ipsilateral LSO have targeted complementary regions within the IC, terminating in alternating sublayers across the extent of the central nucleus (Fig. 6A–D). This complementary pattern is nearly adult-like in its morphology (Shneiderman and Henkel, 1987) and is in place days prior to the functional onset of hearing (in cat P4 = first auditory evoked responses to clicks; P5 = earliest definitive behavioral responses to sound; P7 – P14 = maturation of auditory evoked responses and interaural intensity and phase sensitivities; Cant, 1998). This highly organized arrangement remained consistent throughout the first two postnatal weeks. As described in the unilateral cases, the ipsilateral and contralateral bands appeared to grow slightly in thickness over the first week to ten days, presumably with the growing central nucleus, before reaching their adult dimension of 150 – 200μm. Additionally, there was no evidence of aberrant projections or fibers overshooting their target of the central nucleus. In fact, projection specificity was quite remarkable from the onset, with axons not only recognizing boundaries of the central nucleus, but also restricting themselves to appropriate sublayers as well as the precise nucleotopic region within the central nucleus designated for LSO terminal fields.

Quantification of the separate channels from Figure 6 provided d-values that confirmed a very strong periodicity (Fig. 7); these were not significantly different from values for the crossed and uncrossed inputs in the newborn unilateral experiments (paired t-test p-value = 0.37; p-value > 0.05 suggests means are not significantly different). The uncrossed projection resulted in a d-value = 0.00056, while the crossed projection yielded a d-value of 0.00080. The brightness profiles for the crossed and uncrossed projections produced peaks (arrows, Fig. 7) that were spatially offset from one another (dashed lines, Fig. 7A′, B′), confirming the qualitative findings of alternating periodic projection distributions.

3. Discussion

The present findings indicate that very early in kitten development, projections from LSO to the ipsilateral and contralateral IC course and end parallel to nascent IC layers. By birth, these inputs are dense and already show a banded pattern of distribution in the central nucleus of the IC. Quantitative analysis confirmed the periodic appearance of the two projection distributions. These patterns of interdigitating afferent layers were observed consistently, with the only notable developmental progression being a gradual increase in the thickness of axonal layers over the span of the first two postnatal weeks. While finer-scale rearrangements (e.g. shaping of individual axonal arbors) may well be taking place during this developmental period, these data support the notion that an “adult-like” blueprint of necessary connections is established within the IC in the absence of experience (Gabriele et al., 2000a;Gabriele et al., 2000b). Such an early specificity of multiple afferent projections within the central nucleus could provide the basis for defining the network of functional compartments thought to be responsible for processing midbrain auditory tasks in the adult (Oliver et al., 1997;Loftus et al., 2004).

Measurements and observations regarding the presence of complementary patterns as well as relative band thickness focused exclusively on the dense, narrow axonal laminae. More sparse domains flanking the narrow laminae often extended an additional 50 – 75 μm on either side (refer back to Fig. 6). Thus, while the densest synaptic domains for the crossed and uncrossed pathways were undeniably complementary and exclusive of one another, more peripheral

regions of more sparse distributions exhibited some degree of overlap. It is possible that these regions of sparse overlap may be maintained to adulthood, or, equally likely, they may be further shaped and refined as experience ensues.

3.1 Early segregation of patterned inputs to the central nucleus of the IC

Previous experiments in the adult have described a variety of inputs to the central nucleus of the IC that terminate in a periodic, layered arrangement (Shneiderman and Henkel, 1987;Henkel and Shneiderman, 1988;Oliver et al., 1997;Loftus et al., 2004;Malmierca et al., 2005). Some afferents interdigitate with others (e.g. the crossed and uncrossed LSO projections, Shneiderman and Henkel, 1987;Loftus et al., 2004), whereas other afferents appear to target the same lamina, resulting in a convergence of two separate inputs (e.g. the crossed projections from the LSO and DCN, Oliver et al., 1997; and the uncrossed projections from the MSO and LSO, Loftus et al., 2004). The first study to describe the developmental events leading to the formation of afferent layers within the central nucleus examined a single projection arising from the contralateral DNLL in the embryonic and early postnatal rat (Gabriele et al., 2000a). The crossed DNLL projection invaded first the high-frequency regions and was diffuse, before subsequently invading lower-frequency domains and segregating into the characteristic banded pattern. Although afferent bands were present a week prior to the onset of hearing, they continued to undergo refinement, ultimately yielding the highly specified adult-like patches by P12 (onset of hearing in rat). Similarly, calbindin-positive axonal compartments are present in the newborn cat prior to hearing onset and persist throughout early postnatal development (Henkel et al., 2005). The location of the calbindin-immunostained plexus within the IC as well as the presence and location of calbindin-positive cells in the auditory brainstem suggest that this neurochemical marker is specific for one of the inputs arising from the LSO. Furthermore, labeled LSO projection bands at each age correlated perfectly with that of the reported plexus of calbindin-immunostained fibers (e.g. approximately 75 μm at birth). Although the precise role of these buffering proteins is still unknown, they have been shown to be expressed in a wide variety of neurons (excitatory and inhibitory, long projection and local, fast-responding and slow-responding; Baimbridge et al., 1992). It remains unclear whether this particular marker is specific for the crossed or uncrossed LSO projection. As a general rule, however, different calcium-binding proteins are differentially expressed in separate subpopulations of complementary systems (Baimbridge et al., 1992). Perhaps this is the case for the paired inhibitory and excitatory inputs originating from the LSO. More definitive studies are necessary, however, to determine unequivocally the developing projection pattern that corresponds to calbindin-positive bands, and whether complementary layered inputs may express different calcium-binding proteins like parvalbumin and calretinin.

In the present study, LSO axonal layers were evident at the earliest postnatal stage and exhibited a pattern of distribution similar to that described for the calbindin-immunostained plexus of age-matched kittens (Henkel et al., 2005). In most cases, the ipsilateral and contralateral inputs exhibited a patchy appearance rather than a more immature banded morphology that fills a greater extent of the ventrolateral-to-dorsomedial extent of the target lamina (Gabriele et al., 2000a). While some afferent inputs maintain a banded appearance to adulthood (e.g. the crossed DCN projection), LSO domains exhibit a more restricted or patch-like appearance when mature. Preliminary findings in the postnatal ferret suggest that the same sequence of events described for the DNLL projection (i.e. an initially diffuse input that subsequently segregates into its layered morphology with continued refinement into patches) is also observed for developing LSO axonal layers (Keiger et al., 2003). Additional embryonic experiments are needed to determine whether this same developmental progression that shapes afferent layers from a more widespread terminal field holds true for LSO inputs in the cat. Such experiments would also provide insights regarding the presence or absence of a frequency-related

developmental gradient or whether any initial targeting errors are made by the nascent LSO projections.

The highly organized, layered architecture of projection patterns in the IC is established prior to experience for every afferent system that has been examined to date (the crossed DNLL and the crossed and uncrossed LSO projections). These findings suggest that developmental events intrinsic to the central nucleus help shape the compartmental arrangement of the IC. Based on previously published (Gabriele et al., 2000b) and recent preliminary findings (Gabriele et al., 2005;Shahmoradian et al., 2005) in our laboratory, we now believe that the 'developmental template' that is laid down prior to the onset of hearing is likely established via the interplay of several different developmental mechanisms.

3.2 Potential mechanisms driving early projection specificity

The developmental mechanisms responsible for establishing order from initially complex innervation patterns are often categorized as being activity-dependent or activity-independent processes (Friauf and Lohmann, 1999;Rubel and Cramer, 2002). Prior to the onset of sound-evoked responses, activity-dependent mechanisms involve information encoded as relative levels and patterns of spontaneous activity. The role of spontaneous activity in the construction of patterned projections in the developing visual system (e.g. thalamic eye-specific layers and cortical ocular dominance columns) has been well documented (Stryker and Harris, 1986;Shatz and Stryker, 1988;Sretavan et al., 1988;Katz and Shatz, 1996;Penn et al., 1998;Crowley and Katz, 1999). Spontaneous rhythmic discharges similar to those first described in the retina (Galli and Maffei, 1988;Meister et al., 1991;Wong et al., 1993;Feller et al., 1996;Feller et al., 1997) have now been shown at a variety of levels of the developing auditory system (Lippe, 1994;Kotak and Sanes, 1995;Lippe, 1995;Kros et al., 1998;Jones et al., 2001) and are likely involved in establishing a crude topography and perhaps even some finer aspects of projection specificity. Previously, we determined that removal of the cochlear source of these orchestrated waves of spontaneous activity in neonatal rat influenced the ability of GABAergic DNLL projections to segregate into their characteristic layered arrangements in the IC (Gabriele et al., 2000b). Similar results have been reported for the glycinergic pathway from the MNTB to the LSO, in which decreased levels of primitive activity were shown to prevent the refinement of individual axonal terminal arbors (Sanes and Takacs, 1993). In other systems, activity-dependent mechanisms and competition for synaptic space have been commonly discussed only as they pertain to the predominantly excitatory projections. It is often the case that local circuitry accounts for the vast majority of inhibitory connections. The ascending auditory system, on the other hand, and in particular the array of inputs to the central nucleus of the IC, is inherently different, displaying numerous projection pathways that are inhibitory in nature. Such inhibitory projections, like their neighboring excitatory projections, must achieve a high degree of specificity during early ontogeny and organize into discrete afferent layers (for review see Kandler, 2004). The central nucleus of the IC is therefore unique in that it contains adjacent excitatory and inhibitory projections that may compete within its laminar framework for specific synaptic domains. Interdigitating LSO inputs as presently described could serve as a model system for future experiments testing activity-dependent competitive interactions between neighboring inhibitory (glycinergic, uncrossed LSO) and excitatory (crossed LSO) projection domains.

In addition to these activity-dependent processes, activity-independent mechanisms may also be influential in the early establishment of IC projection patterns. In order for axons to recognize their appropriate targets and subsequently identify a specific subpopulation of neurons with which to form connections, a very precise developmental blueprint must be expressed. It is thought that such a blueprint, that encodes the complex spatial organization of multiple inputs, must involve molecular markers that are capable of cell-cell interactions

(Flanagan and Vanderhaeghen, 1998). One family of receptor tyrosine kinases, the Eph receptors, and their corresponding ligands, the ephrins, may provide the means for such cell-cell communication. These receptor-ligand interactions have been implicated in providing the instructional cues for appropriate construction of complex neural networks in several other systems (visual: Tessier-Lavigne, 1995; striatum: Janis et al., 1999). Eph/ephrin signaling appears to promote axonal segregation in the chick auditory brainstem (for review see Cramer, 2005). In particular, EphA4 signaling is necessary for the appropriate targeting of crossed and uncrossed nucleus magnocellularis inputs onto distinct dendritic regions of nucleus laminaris neurons (Cramer et al., 2004). Similarly, preliminary evidence in our laboratory in rat suggests that certain members of the Eph-ephrin family are transiently expressed in the developing IC (Gabriele et al., 2005;Shahmoradian et al., 2005) in a manner that is spatially and temporally correlated with the initial segregation of layered afferent projections. While our data suggest a compartmentalized expression of these molecular markers, it is also plausible that an environment of overlapping gradients could provide the cues necessary for establishing certain spatial relationships within the IC, not unlike that which has been described previously for the developing retinotectal projection (Cheng et al., 1995;Drescher et al., 1995;Drescher et al., 1997;Hindges et al., 2002;Pittman and Chien, 2002). In conclusion, it is probable that a combination of activity-dependent (e.g. spontaneous activity levels) and activity-independent (e.g. Eph-ephrin receptor-ligand signaling) processes are responsible for ensuring the proper formation of highly organized circuits in the developing auditory system. Future experiments are planned to assess further the roles that competitive interactions and receptor-ligand signaling play in the formation, shaping, and maintenance of patterned auditory projections.

4. Experimental procedures

All animal husbandry and experimental procedures were performed in compliance with the National Institutes of Health “Guide for the Care and Use of Laboratory Animals” (NIH Publications No. 80–23, revised 1996) in facilities accredited by the American Association for the Accreditation of Laboratory Animal Care (AAALAC). Experimental protocols received prior approval by the Institutional Animal Care and Use Committees at James Madison University and Wake Forest University School of Medicine. Results from 20 neonatal cats were compiled in the present study. Due to the difficulty in visualizing lipophilic carbocyanine dyes in pathways that have already been myelinated (preliminary observations, see also Lukas et al., 1998;Hofmann and Bleckmann, 1999), experiments were restricted to time points during the early postnatal period and concentrated on the developmental stages that precede the onset of hearing (hearing onset in cat between P4–P7).

4.1 Labeling of the crossed and uncrossed LSO-IC projections

Anterograde tracing experiments were performed in neonatal kittens at P0 (birth), P4, P7, P10, and P14. At the respective ages, animals were given an overdose of ketamine (40 mg/kg) and xylazine (2 mg/kg) and perfused through the heart with a physiological rinse solution followed by a 4% paraformaldehyde fixative. The brains were removed from the skull and post-fixed with the same fixative for 24–48 hours. Brains then were blocked in the coronal plane just rostral to the superior colliculus and caudal to the cerebellum. The brains were embedded in an egg yolk/gelatin mixture (5 ml 8% gelatin in dH_2O: 10 ml egg yolk), and a cut-down procedure was performed as previously described (Gabriele et al., 2000a;Gabriele et al., 2000b;Gabriele et al., 2006). Briefly, coronal sections were cut on a vibratome (50–75 μm) from caudal to rostral until the caudal extent of the LSO (situated just rostral to the facial nucleus) was identified utilizing darkfield microscopy. Glass pins uniformly coated with the lipophilic dyes, DiI (1,1′-dioctodecyl-3,3,3′,3′-tetramethylindocarbocyanine perchlorate; Invitrogen, Carlsbad, CA) and/or DiD- (1,1′-dioctodecyl-3,3,3′,3′-tetramethylindocarbocyanine perchlorate, 4-chlorobenzenesulfonate salt; Invitrogen,

Carlsbad, CA) were positioned in the left and right LSO, respectively. Previous experience with this approach allowed us to estimate the approximate spread of the dye from the application site in the fixed tissue preparations. Pins were positioned in the center of the LSO such that the radial spread of the dye filled the LSO without significant leaching into the neighboring MSO or periolivary regions. Following pin placements, the block was placed in fresh 4% paraformaldehyde fixative and incubated in the dark at 37°C (Lukas et al., 1998;Gabriele et al., 2000a;Gabriele et al., 2000b). Fixative was changed monthly during the incubation period. After allowing 2–3 months for the diffusion of the dye, the blocks were removed from the dark, and the pins were removed prior to sectioning. The remaining tissue block was then sectioned on a vibratome (50–75 μm) in the coronal plane and counterstained prior to mounting. To provide a reference for labeled axonal layers within the central nucleus, the majority of cases were counterstained with bis-benzimide, a fluorescent nuclear counterstain (Hoechst 33258; Invitrogen, Carlsbad, CA). In the remaining cases a Nissl counterstain was used on alternate sections. All fluorescent material was ultimately mounted onto microscope slides and coverslipped while still wet with GelMount (BioMeda, Foster City, CA). After one hour, slides were permanently sealed using Cytoseal (Stephens Scientific, Riverdale, NJ) and stored in the dark at 4°C. Nissl-stained sections were mounted on gelatin-subbed slides, dehydrated, and cleared before coverslipping with Cytoseal.

4.2 Fluorescence microscopy, image acquisition, and deconvolution

Sections were viewed using epifluorescence on two systems (Zeiss Axioskop, Nikon C1si). Both imaging setups were equipped with an R and B Phycoerythrin filter set (for DiI visualization), a Cy5 filter set (for DiD visualization), and a DAPI filter set (for bis-benzimide visualization). Optimized filter sets were designed by Chroma Technology (Brattleboro, VT) for the unequivocal visualization of the two tracers and the fluorescent nuclear stain. To document the developmental progression in the shaping of LSO axonal layers, monochrome digital images were captured at standardized serial spaced levels throughout the rostrocaudal extent of the central nucleus. Image capturing was performed using a SPOT RT slider digital camera (Diagnostic Instruments, Sterling Heights, MI). Raw grayscale images were acquired with SPOT software and saved as uncompressed TIFF files. Raw image files then were filtered using a 2-D blind deconvolution algorithm (Autoquant Imaging, Inc, Watervliet, NY). For color and merged digital image files, grayscale images were imported into Adobe Photoshop and pseudocolored (DiI = red channel; DiD = green channel; bis-benzimide = blue channel; Adobe Systems Inc., San Jose, CA). Finally, brightness and contrast values may have been adjusted slightly in some cases for illustration purposes.

4.3 Quantitative assessment of periodicity and thickness of labeled projection patterns

Digitized images of sections at comparable levels of the central nucleus were imported into Scion NIH Image software (Scion Corp., http://www.scioncorp.com/) to compare the periodic spacing of labeled projections in the coronal plane at the various developmental stages. All images were converted to grayscale and inverted (inverting the images facilitated viewing bands and interband spaces as peaks and troughs respectively on the generated brightness plot profiles). A consistent rectangular area was defined for sampling along the tonotopic axis, orthogonal to the orientation of the labeled axonal layers. Briefly, utilizing a bis-benzimide counterstain to delineate the major subdivisions of the IC, the total distance of the central nucleus from its ventrolateral margin to its dorsomedial boundary with the dorsal cortex was measured in each section. This total dimension was divided into thirds, and the standardized rectangular sampling area was oriented such that it occupied the defined middle domain. The defined area was then rotated to achieve a vertical, columnar orientation for the labeled afferent layers. A brightness profile function was performed such that each data point on the generated graph reflected an average grayscale value for all the points in a single column of pixels. A statistical autocorrelation algorithm (IGOR Pro software, WaveMetrics, Inc., Lake Oswego,

OR) was performed on the raw brightness profile values to extract any periodicity in the data set. A Durbin-Watson test yielded d-values that were utilized as a standard for assessing the relative bandedness of a given projection pattern. Maximal (d-value tending to 0) and minimal levels (d-value tending to 1) of bandedness were initially determined by running a Durbin-Watson test on (1) an artificially rendered banded control image file, and (2) a homogeneous, non-banded control image file. To determine the d-value that represented the strongest periodicity, an artificial periodic pattern was generated by replicating and aligning a cropped portion of the most clearly defined adjacent band and interband space from our image library. A Durbin-Watson test for this artificially generated periodicity provided a d-value equal to 0.00058. Conversely, a homogenous nuclear stain of the central nucleus showing no evidence of a layered arrangement was analyzed with the same statistical measures to provide a baseline for data exhibiting little to no periodicity (d-value equal to 0.99946). These control d-values provided a means for comparing relative levels of bandedness based on d-values generated from other data images. The d-values of the banded and non-banded controls simply provide ends of a general d-value spectrum of periodicity, and it remains a distinct possibility that certain cases may exceed these d-value standards as defined by these controls.

Additionally, band thickness, or the band dimension perpendicular to the orientation of the layers in a coronal section (Henkel et al., 2003), was measured to determine whether any growth or refinement of axonal layers takes place during the first two postnatal weeks. Given the sometimes patchy and non-uniform morphology of bands within the defined rectangular periodicity sample, prominent bands from our raw images were qualitatively identified and measured, and an approximate range for band thickness at each age was determined.

Acknowledgements

The authors would like to thank RL Fathke for insightful discussions pertaining to the present findings and for his valuable comments on the manuscript. This work was sponsored by USPHS grant NIH NS35008 (JGM), NSF-MRI DBI-0619207 (MLG) and Jeffress Memorial Trust Grant No. J-665 (MLG). Some of the current material came from tissue blocks harvested from previously published experiments (Gabriele et al., 2006) funded in part by NS36916 (Barry E. Stein) Special funds also provided by the Mr. & Mrs. Siebert Neuroscience Endowment.

GRANT SPONSOR: NIH (NINDS), NSF-MRI, Jeffress Memorial Trust

GRANT NUMBERS: NS35008, NS36916, DBI-0619207, J-665

Literature References

Adams JC. Ascending projections to the inferior colliculus. J Comp Neurol 1979;183:519–538. [PubMed: 759446]

Baimbridge KG, Celio MR, Rogers JH. Calcium-binding proteins in the nervous system. Trends Neurosci 1992;15:303–308. [PubMed: 1384200]

Beyerl BD. Afferent projections to the central nucleus of the inferior colliculus in the rat. Brain Res 1978;145:209–223. [PubMed: 638786]

Brunso-Bechtold JK, Thompson GC, Masterton RB. HRP study of the organization of auditory afferents ascending to central nucleus of inferior colliculus in cat. J Comp Neurol 1981;197:705–722. [PubMed: 7229134]

Cant, NB. Structural development of the mammalian auditory pathways. In: Rubel, EW.; Popper, AN.; Fay, RR., editors. Development of the Auditory System. Springer-Verlag; New York: 1998. p. 315-413.

Cheng HJ, Nakamoto M, Bergemann AD, Flanagan JG. Complementary gradients in expression and binding of ELF-1 and Mek4 in development of the topographic retinotectal projection map. Cell 1995;82:371–381. [PubMed: 7634327]

Cramer KS. Eph proteins and the assembly of auditory circuits. Hear Res 2005;206:42–51. [PubMed: 16080997]

Cramer KS, Bermingham-McDonogh O, Krull CE, Rubel EW. EphA4 signaling promotes axon segregation in the developing auditory system. Dev Biol 2004;269:26–35. [PubMed: 15081355]

Crowley JC, Katz LC. Development of ocular dominance columns in the absence of retinal input. Nat Neurosci 1999;2:1125–1130. [PubMed: 10570491]

Drescher U, Bonhoeffer F, Muller BK. The Eph family in retinal axon guidance. Curr Opin Neurobiol 1997;7:75–80. [PubMed: 9039788]

Drescher U, Kremoser C, Handwerker C, Loschinger J, Noda M, Bonhoeffer F. In vitro guidance of retinal ganglion cell axons by RAGS, a 25 kDa tectal protein related to ligands for Eph receptor tyrosine kinases. Cell 1995;82:359–370. [PubMed: 7634326]

Elverland HH. Ascending and intrinsic projections of the superior olivary complex in the cat. Exp Brain Res 1978;32:117–134. [PubMed: 658183]

Faye-Lund H, Osen KK. Anatomy of the inferior colliculus in rat. Anat Embryol (Berl) 1985;171:1–20. [PubMed: 3985354]

Feller MB, Butts DA, Aaron HL, Rokhsar DS, Shatz CJ. Dynamic processes shape spatiotemporal properties of retinal waves. Neuron 1997;19:293–306. [PubMed: 9292720]

Feller MB, Wellis DP, Stellwagen D, Werblin FS, Shatz CJ. Requirement for cholinergic synaptic transmission in the propagation of spontaneous retinal waves. Science 1996;272:1182–1187. [PubMed: 8638165]

Flanagan JG, Vanderhaeghen P. The ephrins and Eph receptors in neural development. Annu Rev Neurosci 1998;21:309–345. [PubMed: 9530499]

Franklin S, Brunso-Bechtold JK, Henkel CK. Competitive interaction shapes development of afferent segregation in banded projections from the dorsal nucleus of the lateral lemniscus to the inferior colliculus. Assoc for Res Otolaryngol Abstr 2005;28:695.

Friauf E, Lohmann C. Development of auditory brainstem circuitry. Activity-dependent and activity-independent processes. Cell Tissue Res 1999;297:187–195. [PubMed: 10470488]

Gabriele ML, Brunso-Bechtold JK, Henkel CK. Development of afferent patterns in the inferior colliculus of the rat: projection from the dorsal nucleus of the lateral lemniscus. J Comp Neurol 2000a;416:368–382. [PubMed: 10602095]

Gabriele ML, Brunso-Bechtold JK, Henkel CK. Plasticity in the development of afferent patterns in the inferior colliculus of the rat after unilateral cochlear ablation. J Neurosci 2000b;20:6939–6949. [PubMed: 10995838]

Gabriele ML, Robenolt JL, Laz AA. Involvement of ephrins and Eph receptors in establishing early pattern formation in the auditory midbrain. Assoc for Res Otolaryngol Abstr 2005;28:690.

Gabriele ML, Smoot JE, Jiang H, Stein BE, McHaffie JG. Early establishment of adult-like nigrotectal architecture in the neonatal cat: a double-labeling study using carbocyanine dyes. Neuroscience 2006;137:1309–1319. [PubMed: 16359814]

Galli L, Maffei L. Spontaneous impulse activity of rat retinal ganglion cells in prenatal life. Science 1988;242:90–91. [PubMed: 3175637]

Henkel CK, Fuentes-Santamaria V, Alvarado JC, Brunso-Bechtold JK. Quantitative measurement of afferent layers in the ferret inferior colliculus: DNLL projections to sublayers. Hear Res 2003;177:32–42. [PubMed: 12618315]

Henkel CK, Gabriele ML, McHaffie JG. Quantitative assessment of developing afferent patterns in the cat inferior colliculus revealed with calbindin immunohistochemistry and tract tracing methods. Neuroscience 2005;136:945–955. [PubMed: 16344162]

Henkel CK, Shneiderman A. Nucleus sagulum: projections of a lateral tegmental area to the inferior colliculus in the cat. J Comp Neurol 1988;271:577–588. [PubMed: 2454973]

Henkel CK, Spangler KM. Organization of the efferent projections of the medial superior olivary nucleus in the cat as revealed by HRP and autoradiographic tracing methods. J Comp Neurol 1983;221:416–428. [PubMed: 6319460]

Hindges R, McLaughlin T, Genoud N, Henkemeyer M, O'Leary DD. EphB forward signaling controls directional branch extension and arborization required for dorsal-ventral retinotopic mapping. Neuron 2002;35:475–487. [PubMed: 12165470]

Hofmann MH, Bleckmann H. Effect of temperature and calcium on transneuronal diffusion of DiI in fixed brain preparations. J Neurosci Methods 1999;88:27–31. [PubMed: 10379576]

Janis LS, Cassidy RM, Kromer LF. Ephrin-A binding and EphA receptor expression delineate the matrix compartment of the striatum. J Neurosci 1999;19:4962–4971. [PubMed: 10366629]

Jones TA, Jones SM, Paggett KC. Primordial rhythmic bursting in embryonic cochlear ganglion cells. J Neurosci 2001;21:8129–8135. [PubMed: 11588185]

Kandler K. Activity-dependent organization of inhibitory circuits: lessons from the auditory system. Curr Opin Neurobiol 2004;14:96–104. [PubMed: 15018944]

Kandler K, Friauf E. Pre- and postnatal development of efferent connections of the cochlear nucleus in the rat. J Comp Neurol 1993;328:161–184. [PubMed: 8423239]

Katz LC, Shatz CJ. Synaptic activity and the construction of cortical circuits. Science 1996;274:1133–1138. [PubMed: 8895456]

Kotak VC, Sanes DH. Synaptically evoked prolonged depolarizations in the developing auditory system. J Neurophysiol 1995;74:1611–1620. [PubMed: 8989397]

Keiger CJ, Henkel CK, Brunso-Bechtold JK. Normal postnatal development of banded afferent projections to the inferior colliculus of the ferret from the superior olivary complex. Assoc for Res Otolaryngol Abstr 2005;26:145–146.

Kros CJ, Ruppersberg JP, Rusch A. Expression of a potassium current in inner hair cells during development of hearing in mice. Nature 1998;394:281–284. [PubMed: 9685158]

Kudo M. Projections of the nuclei of the lateral lemniscus in the cat: an autoradiographic study. Brain Res 1981;221:57–69. [PubMed: 6168337]

Lippe WR. Relationship between frequency of spontaneous bursting and tonotopic position in the developing avian auditory system. Brain Res 1995;703:205–213. [PubMed: 8719634]

Lippe WR. Rhythmic spontaneous activity in the developing avian auditory system. J Neurosci 1994;14:1486–1495. [PubMed: 8126550]

Loftus WC, Bishop DC, Saint Marie RL, Oliver DL. Organization of binaural excitatory and inhibitory inputs to the inferior colliculus from the superior olive. J Comp Neurol 2004;472:330–344. [PubMed: 15065128]

Lukas JR, Aigner M, Denk M, Heinzl H, Burian M, Mayr R. Carbocyanine postmortem neuronal tracing. Influence of different parameters on tracing distance and combination with immunocytochemistry. J Histochem Cytochem 1998;46:901–910. [PubMed: 9671441]

Malmierca MS, Saint Marie RL, Merchan MA, Oliver DL. Laminar inputs from dorsal cochlear nucleus and ventral cochlear nucleus to the central nucleus of the inferior colliculus: two patterns of convergence. Neuroscience 2005;136:883–894. [PubMed: 16344158]

Meister M, Wong RO, Baylor DA, Shatz CJ. Synchronous bursts of action potentials in ganglion cells of the developing mammalian retina. Science 1991;252:939–943. [PubMed: 2035024]

Merzenich MM, Reid MD. Representation of the cochlea within the inferior colliculus of the cat. Brain Res 1974;77:397–415. [PubMed: 4854119]

Morest DK. The laminar structure of the inferior colliculus of the cat. Anat Rec 1964;148:314.

Morest DK, Oliver DL. The neuronal architecture of the inferior colliculus in the cat: defining the functional anatomy of the auditory midbrain. J Comp Neurol 1984;222:209–236. [PubMed: 6699208]

Okoyama S, Moriizumi T, Kitao Y, Kawano J, Kudo M. Postnatal development of the projection from the medial superior olive to the inferior colliculus in the rat. Hear Res 1995;88:65–70. [PubMed: 8576005]

Oliver DL. Dorsal cochlear nucleus projections to the inferior colliculus in the cat: A light and electron microscopic study. J Comp Neurol 1984;224:155–172.

Oliver DL. Projections to the inferior colliculus from the anteroventral cochlear nucleus in the cat: possible substrates for binaural interaction. J Comp Neurol 1987a;264:24–46. [PubMed: 2445792]

Oliver DL. Projections to the inferior colliculus from the anteroventral cochlear nucleus in the cat: possible substrates for binaural interaction. J Comp Neurol 1987b;264:24–46. [PubMed: 2445792]

Oliver, DL. Neuronal organization in the inferior colliculus. In: Winer, JA.; Schreiner, CE., editors. The Inferior Colliculus. Springer-Verlag; New York: 2005. p. 69-114.

Oliver DL, Beckius GE, Bishop DC, Kuwada S. Simultaneous anterograde labeling of axonal layers from lateral superior olive and dorsal cochlear nucleus in the inferior colliculus of cat. J Comp Neurol 1997;382:215–229. [PubMed: 9183690]

Oliver DL, Beckius GE, Shneiderman A. Axonal projections from the lateral and medial superior olive to the inferior colliculus of the cat: a study using electron microscopic autoradiography. J Comp Neurol 1995;360:17–32. [PubMed: 7499562]

Oliver, DL.; Huerta, MF. Inferior and superior colliculi. In: Webster, DB.; Popper, AN.; Fay, RR., editors. The Mammalian Auditory Pathway. Springer-Verlag; New York: 1992. p. 168-221.

Oliver DL, Morest DK. The central nucleus of the inferior colliculus in the cat. J Comp Neurol 1984;222:237–264. [PubMed: 6699209]

Osen KK. Projection of the cochlear nuclei on the inferior colliculus in the cat. J Comp Neurol 1972;144:355–372. [PubMed: 5027335]

Penn AA, Riquelme PA, Feller MB, Shatz CJ. Competition in retinogeniculate patterning driven by spontaneous activity. Science 1998;279:2108–2112. [PubMed: 9516112]

Pittman A, Chien CB. Understanding dorsoventral topography: backwards and forwards. Neuron 2002;35:409–411. [PubMed: 12165462]

Roth GL, Aitkin LM, Andersen RA, Merzenich MM. Some features of the spatial organization of the central nucleus of the inferior colliculus of the cat. J Comp Neurol 1978;182:661–680. [PubMed: 721973]

Rubel EW, Cramer KS. Choosing axonal real estate: location, location, location. J Comp Neurol 2002;448:1–5. [PubMed: 12012372]

Sanes DH, Takacs C. Activity-dependent refinement of inhibitory connections. Eur J Neurosci 1993;5:570–574. [PubMed: 8261131]

Schreiner CE, Langner G. Laminar fine structure of frequency organization in auditory midbrain. Nature 1997;388:383–386. [PubMed: 9237756]

Semple MN, Aitkin LM. Representation of sound frequency and laterality by units in central nucleus of cat inferior colliculus. J Neurophysiol 1979;42:1626–1639. [PubMed: 501392]

Shahmoradian SH, James RL, Simpson NS, Gabriele ML. Banded ephrin-B3 expression patterns in the neonatal rat inferior colliculus. Soc for Neurosci Abstr 2005;35:942.2.

Shatz CJ, Stryker MP. Prenatal tetrodotoxin infusion blocks segregation of retinogeniculate afferents. Science 1988;242:87–89. [PubMed: 3175636]

Shneiderman A, Henkel CK. Banding of lateral superior olivary nucleus afferents in the inferior colliculus: a possible substrate for sensory integration. J Comp Neurol 1987;266:519–534. [PubMed: 2449472]

Shneiderman A, Oliver DL, Henkel CK. Connections of the dorsal nucleus of the lateral lemniscus: an inhibitory parallel pathway in the ascending auditory system? J Comp Neurol 1988;276:188–208. [PubMed: 3220980]

Sretavan DW, Shatz CJ, Stryker MP. Modification of retinal ganglion cell axon morphology by prenatal infusion of tetrodotoxin. Nature 1988;336:468–471. [PubMed: 2461517]

Stryker MP, Harris WA. Binocular impulse blockade prevents the formation of ocular dominance columns in cat visual cortex. J Neurosci 1986;6:2117–2133. [PubMed: 3746403]

Tanaka K, Otani K, Tokunaga A, Sugita S. The organization of neurons in the nucleus of the lateral lemniscus projecting to the superior and inferior colliculi in the rat. Brain Res 1985;341:252–260. [PubMed: 4041794]

Tessier-Lavigne M. Eph receptor tyrosine kinases, axon repulsion, and the development of topographic maps. Cell 1995;82:345–348. [PubMed: 7634322]

Wong RO, Meister M, Shatz CJ. Transient period of correlated bursting activity during development of the mammalian retina. Neuron 1993;11:923–938. [PubMed: 8240814]

Zook JM, Casseday JH. Convergence of ascending pathways at the inferior colliculus of the mustache bat, Pteronotus parnellii. J Comp Neurol 1987;261:347–361. [PubMed: 3611416]

Zook JM, Casseday JH. Origin of ascending projections to inferior colliculus in the mustache bat, Pteronotus parnellii. J Comp Neurol 1982;207:14–28. [PubMed: 7096636]

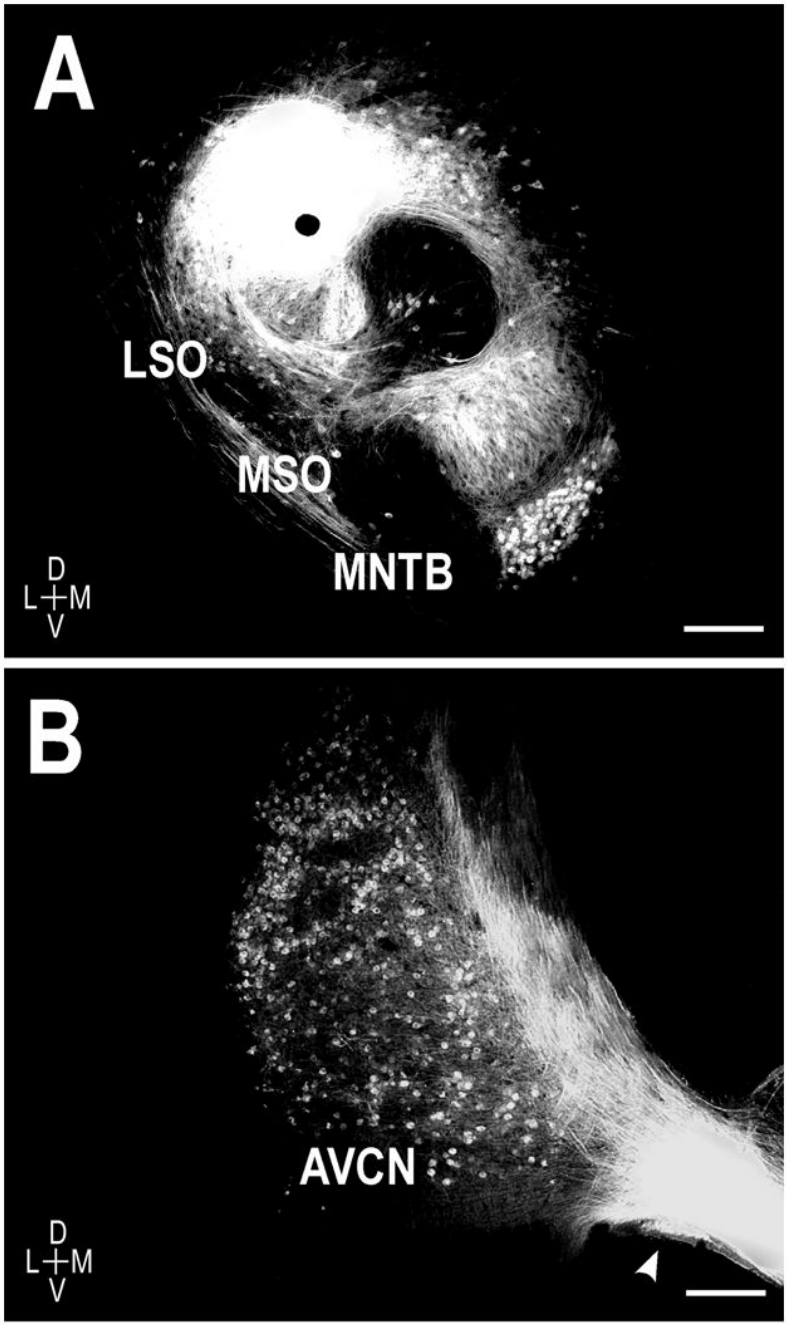

Figure 1.

Representative DiI placement in a P0 unilateral case. A. Deposits of DiI were placed in the left LSO, resulting in anterograde labeling of the crossed and uncrossed LSO projections to the IC. Note the retrogradely-labeled principal cells of the MNTB. B. Evidence of retrograde labeling of the spherical bushy cell population in the ipsilateral AVCN of a different animal following LSO dye placement. *D* = dorsal, *V* = ventral, *L* = lateral, *M* = medial. Scale bars = 250 μm.

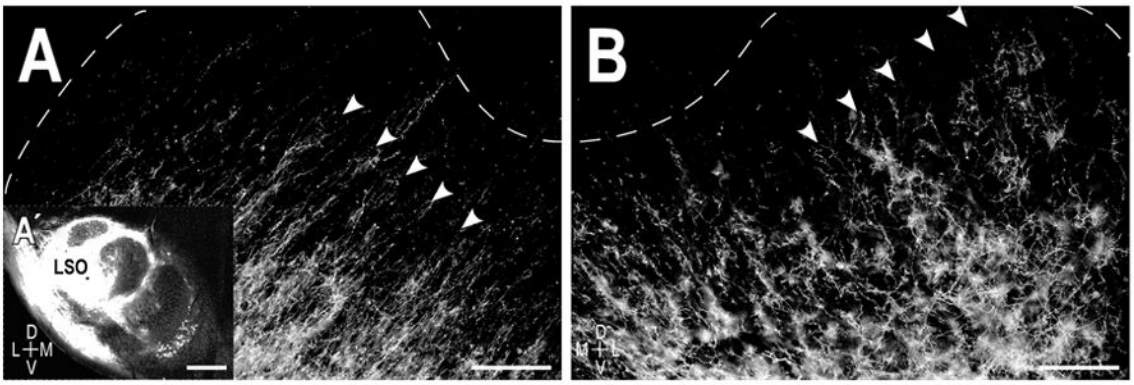

Figure 2.
Resultant afferent labeling in the central nucleus of the IC in a P0 cat. A. Axonal layers (arrowheads) in the left IC ipsilateral to the LSO dye placement (A′ inset). B. Labeled axons in the contralateral IC exhibited a similar laminar bias, forming a periodic pattern of afferent bands (arrowheads) that spanned the frequency axis of the central nucleus. Dashed contours delineate boundaries of the central nucleus with the dorsal cortex and the external cortex as determined by the counterstaining. Scale bars A, B = 200 μm, A′ = 500 μm.

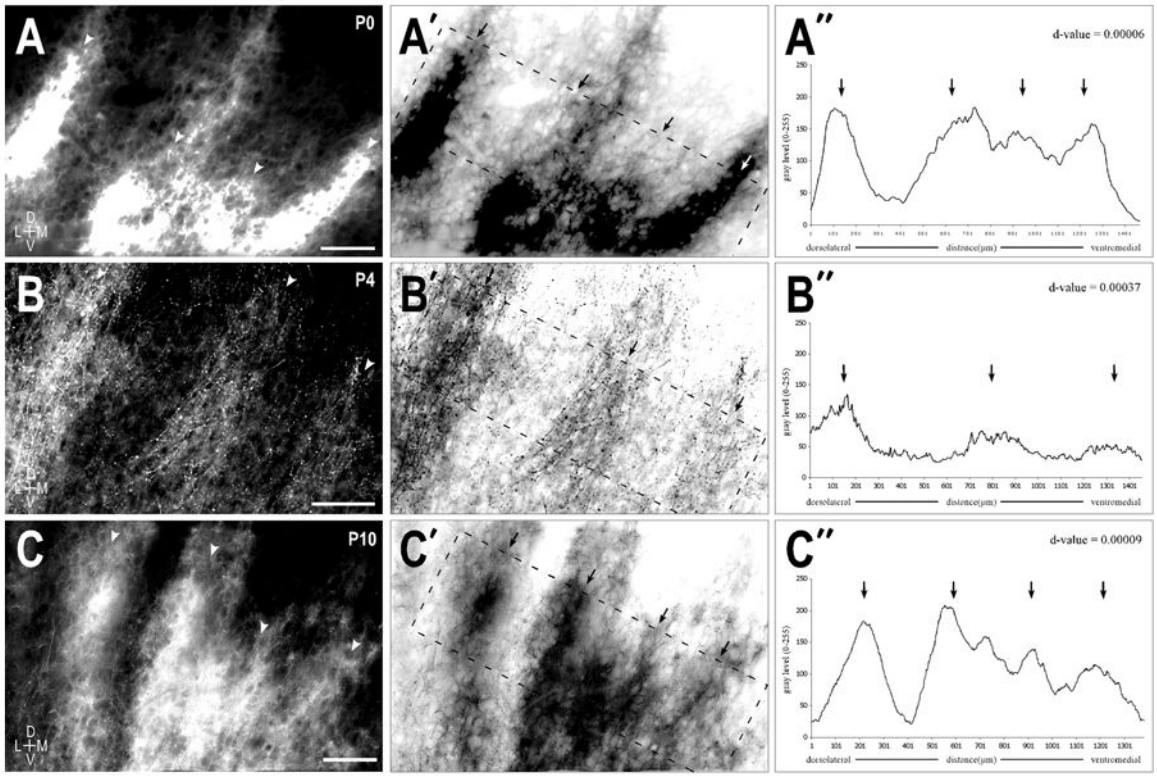

Figure 3.

Uncrossed LSO afferent layers at P0 (A series), P4 (B series), and P10 (C series). A. Fluorescent micrograph of prominent axonal layers (arrowheads) in the left IC at birth. A′. Inverted image of (A) highlighting the area (dashed rectangle) used to generate the brightness plot profile shown in (A″). A″. Brightness profile graph where peaks correspond to afferent dense areas (arrows) and troughs correspond to less dense interband spaces. Layers within the rectangular sample were rotated to vertical to facilitate quantification of the bands in an averaged columnar fashion. A Durbin-Watson statistical autocorrelation test was performed on the raw brightness profile values to extract any periodicity in the data set. B & C series. Same progression as described for the A series. The resultant d-values tending to 0 were indicative of a very strong periodicity at each of these early postnatal stages. Scale bars = 100 μm.

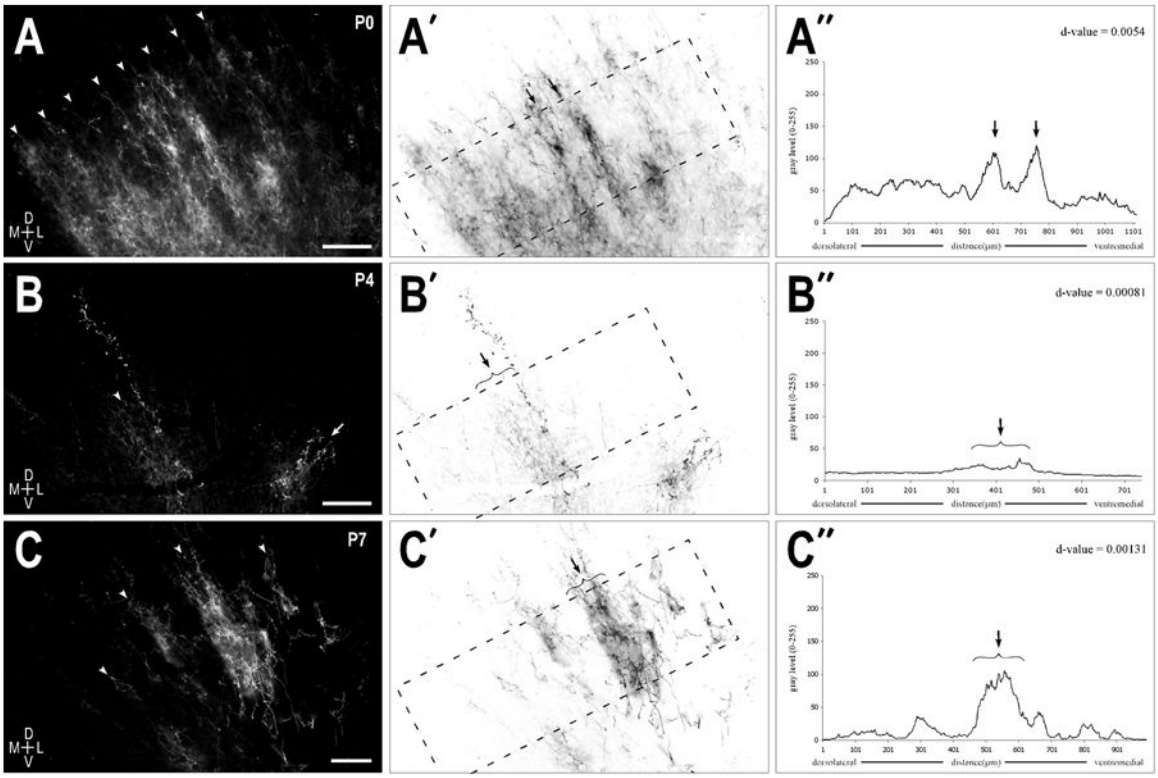

Figure 4.

Crossed LSO afferent layers at P0 (A series), P4 (B series), and P7 (C series). A. Alternating axonal layers (arrowheads) in the right IC at birth following a large dye placement in the contralateral LSO. A′. Inverted image of (A) highlighting the area (dashed rectangle) used to generate the brightness plot profile shown in (A″). A″. Raw brightness profile data showing prominent afferent bands (arrows) and a distribution pattern that again produced a d-value (0.0054) suggestive of a strong periodicity. B & C series. Same progression as described for the A series. Dye placements in the contralateral LSO for (B) and (C) were more localized than in (A), thereby yielding fewer afferent layers in the central nucleus of the IC. Autocorrelative d-values again indicated the presence of a strong periodicity in the distributions patterns of the crossed LSO projection throughout the first postnatal week. Scale bars = 150 μm.

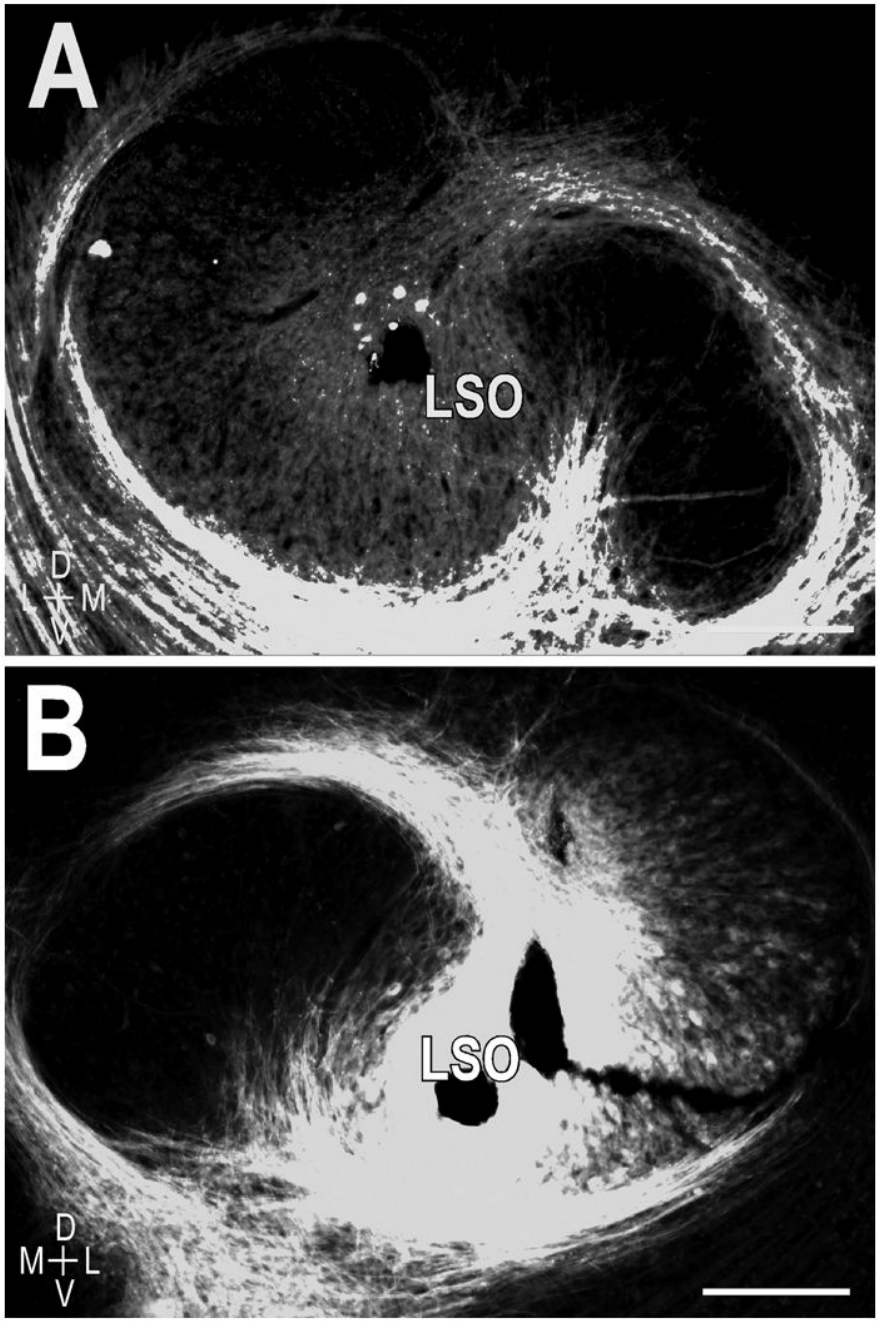

Figure 5.
Anterograde dye placements for double-labeling experiments. Lipophilic carbocyanine dyes DiI and DiD positioned bilaterally in the LSO. A. DiI (red) placement in the center of the left LSO with a nuclear bis-benzimide stain (blue) for reference. B. DiD (green) placement centered in the corresponding frequency representation of the right LSO. Scale bars = 200 μm.

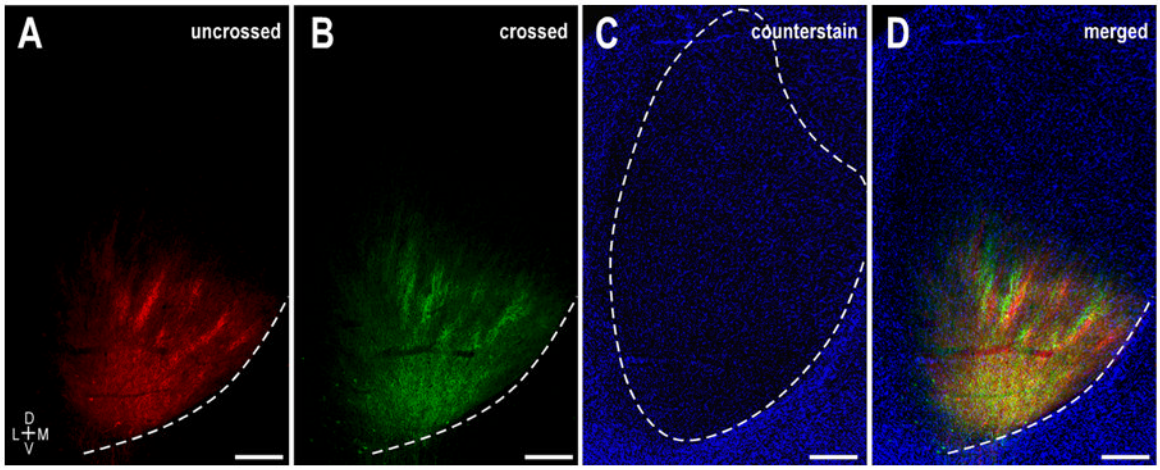

Figure 6.

Interdigitation of crossed and uncrossed LSO axonal layers in the left IC at P0. A. DiI labeling illustrating ipsilateral LSO bands. B. Same field as (A) showing DiD label arising from the contralateral LSO. C. Pseudocolored image of a Nissl stain of the same field of view highlighting boundaries of the central nucleus (dashed contour). D. Digitally merged illustration of (A – C) showing the spatial relationship of uncrossed and crossed LSO projection domains within the central nucleus of the IC. Dashed contours in A, B, and D depict the ventromedial border of the IC. Scale bars = 500 μm.

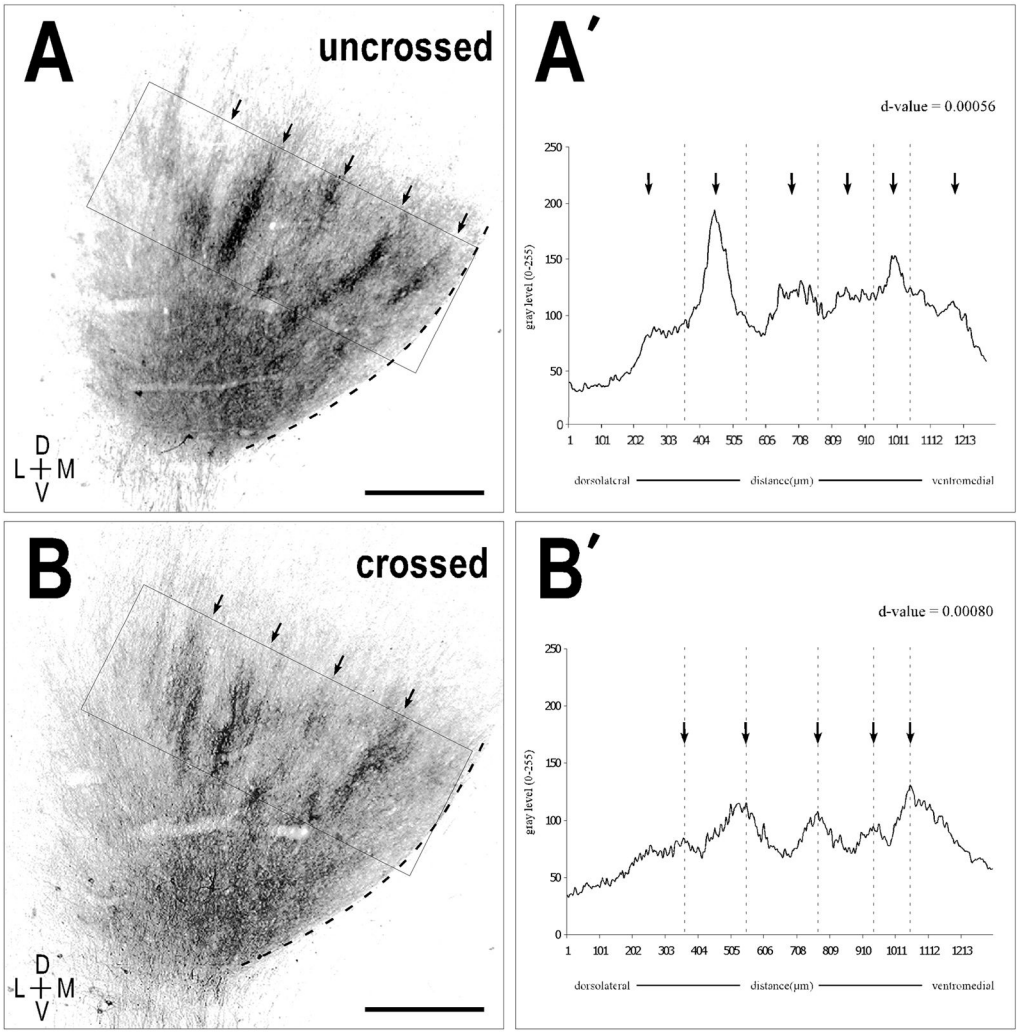

Figure 7.

Quantitative assessment of periodicity of crossed and uncrossed projections in a bilateral P0 case. A, B. Monochrome, inverted images of (Fig. 6A, 6B respectively) highlighting the areas (solid rectangles) used to generate the brightness plot profiles shown in (A′, B′). Prominent axonal layers (arrows) in images correspond to peaks in the plot profile (arrows). A′, B′. Autocorrelation analysis again revealed a strong periodic component for both the uncrossed and crossed projection patterns (d-values equal to 0.00056 and 0.00080, respectively). Note that defined peaks (dashed vertical lines) of the crossed projection are spatially offset with that of the major peaks in the brightness plot profile for the uncrossed projection. Scale bars = 500 μm.